Sakarya University Journal of Computer and Information Sciences
http://saucis.sakarya.edu.tr/

DOI: 10.35377/saucis...1391813 RESEARCH ARTICLE

Performance Evaluation of OTFS-NOMA Scheme for High Mobility Users

İnci Umakoğlu [1], Mustafa Namdar [1], Arif Başgümüş [2]

[1] Department of Electrical and Electronics Engineering, Kütahya Dumlupınar University, Kütahya, Türkiye
[2] Department of Electrical and Electronics Engineering, Bursa Uludağ University, Bursa, Türkiye

Corresponding author:
Inci Umakoglu, Department of Electrical and Electronics Engineering Kutahya Dumlupinar University
E-mail address:
inci.umakoglu@dpu.edu.tr

Submitted: 16 November 2023
Revision Requested: 29 November 2023
Last Revision Received: 30 November 2023
Accepted: 20 December 2023
Published Online: 27 December 2023

Citation: İ. Umakoğlu, M. Namdar, and A. Başgümüş, Performance Evaluation of OTFS-NOMA Scheme for High Mobility Users. *Sakarya University Journal of Computer and Information Sciences*. 6 (3) https://doi.org/10.35377/saucis...1391813

ABSTRACT

Orthogonal Time Frequency Space (OTFS) is a promising approach which is widely employed in sixth generation (6G) wireless network systems. Because of its superior performance in high-mobility environments, OTFS modulation has received a lot of attention lately. Due to OTFS modulation works in the delay-Doppler (DD) domain rather than the conventional time-frequency (TF) domain, it works effectively in such circumstances. The idea of non-orthogonal multiple access (NOMA) is integrated into OTFS as an important approach to improve the spectral efficiency (SE) to investigate the efficiency potential and performance. In this research, we study OTFS modulated NOMA system for two destination users in the high mobility environment. The message passing detection algorithm is utilized to examine bit error rate (BER) performance for both near and far users in the proposed OTFS modulated NOMA system. The BER simulation results demonstrate that the power allocation (PA) coefficient, delays, and Doppler effects significantly impact the performance of the system. It is observed that the performance of the far user did not drop below a particular BER level. The BER value for the U_1 user is 0.1, while the BER value for the U_2 user is nearly 0.25 at 10 dB SNR, resulting in a 2.5 times better BER performance in the 4-QAM scenario. The BER value is about 0.27 for the U_1 user, while the BER value for the U_2 user is approximately 0.33 at 10 dB SNR in the 16-QAM approach. It is concluded that the Doppler effect causes BER performance degradation for both users.

Keywords: Bit Error Rate, Doppler Effect, NOMA, OTFS

1. Introduction

Non-orthogonal multiple access (NOMA) is accepted as an important multiplexing approach for new generation wireless networks. The concept of NOMA is to improve the spectral efficiency (SE) of fifth generation (5G) and beyond communication networks. NOMA provides different power levels to multiple users at the same time in the same frequency band. Successive interference cancellation (SIC) is carried out in NOMA to decode incoming message information at the receiver side. As opposed to conventional orthogonal multiple access (OMA) methods, NOMA is a methodology that can offer higher SE performance, lower latency and maintain user fairness. Scenarios with quality of service requirements or varying channel conditions are grouped together for users with low-speed mobility in studies [1]–[3]. Numerous communication networks, including millimeter wave networks, multi-input multiple-output networks, and visible light communication systems are utilized with NOMA techniques.

Wireless communication is the area of the communication industry that is growing most rapidly. The demand for research beyond 5G and sixth generation (6G) is growing daily as scientists and researchers realize that new wireless communication techniques have to be developed for the growth of future infrastructure. Reliable communication is anticipated to be enabled in both time-invariant and time-variant wireless channels. It is difficult to meet the ever-increasing needs of 6G. Traditional orthogonal frequency-division multiplexing (OFDM) modulation, which has been widely utilized in 5G cellular networks, is susceptible to the high Doppler effect. The 5G methodologies and specifications are insufficient to fulfill the demands of future applications. The objective of sixth generation mobile technology is to improve communication in scenarios with high-speed mobility, such as vehicle-to-everything, Internet of Things, unmanned aerial vehicles, and high-speed rail. Orthogonal frequency division multiplexing (OFDM) is a very popular

This work is licensed under Creative Commons Attribution-NonCommercial 4.0 International License

solution for 4G and 5G wireless networks. OFDM is developed specifically to avoid inter-symbol interference due to the channel's time dispersion. Nonetheless, because of the Doppler effect, subcarriers are no longer orthogonal and intercarrier interference occurs in OFDM. Therefore, this causes severe performance degradations and OFDM is no longer robust in high-speed mobility environments [4]. To enhance the system performance and the SE of OFDM, numerous alternative multicarrier waveforms have been studied, including unified filter multicarrier, filter bank multicarrier, and generalized frequency-division multiplexing. The aforementioned waveforms, however, have been designed for low-mobility channels and would significantly degrade in performance when employed in high-mobility conditions because of the negative impact of a strong Doppler effect. Recently, the orthogonal time-frequency-space (OTFS) waveform has been proposed as a way of avoiding the limitation of OFDM in time-varying channels. OTFS has the benefit of allowing time-invariant channel gains to be used in the delay-Doppler (DD) domain in contrast to conventional modulation techniques such as OFDM. In conditions of high-speed mobility, this makes signal detection and channel estimation simpler. OTFS transmits information symbols in the DD domain as opposed to OFDM, which delivers in the time frequency (TF) domain. By doing this, a time-varying channel becomes time-invariant, ensuring that the frequency and time selectivity have the same effect on all symbols in the DD domain.

The methods that are proposed currently in the literature are usually categorized as either OMA or NOMA. Because of user multiplexing in the DD domain, only one user can have access to a given resource block in OTFS-OMA. However, due to Doppler spread, users suffer from multi-user interference. This interference is eliminated by adding guard bands between the destination users. Nevertheless, this leads to a loss of SE [5]. As an alternative approach, OTFS-NOMA allows users to utilize the same resource block. This is the reason underlying the latest suggestions in the literature for power domain [6], [7], and code domain [8], [9] multiplexed OTFS-NOMA system models. In this study, we concentrate on the power domain OTFS-NOMA. This study investigates its applicability to a communication environment in which users have profiles of high-speed mobility. OTFS modulation is used due to its performance in scenarios with doubly selective channels. OTFS utilizes the DD domain by placing users' signals orthogonally. In this study, a two-user downlink OTFS-NOMA system bit error rate (BER) performance is presented. The message transmission (MP) detection technique, which makes use of the DD channel's sparseness, is used at the receiver to accomplish symbol detection. By employing a sparse factor graph-based Gaussian approximation of the interference terms, this method significantly decreases complexity.

Future vehicular networks, underwater acoustic communications (UACs), non-terrestrial networks (NTN), as well as Millimeter-wave and Terahertz communication, all common wireless communication scenarios especially for the feasibility of high-speed mobility scenarios in 6G wireless networks find OTFS to be a desirable option due to its advantageous robustness to the Doppler effect. In addition to being resistant to time-varying channels, it also has a lower peak-to-average power ratio than its OFDM equivalent. Owing to its strong OFDM compatibility, OTFS is also a strong alternative for 6G communication systems.

Especially, BER performances have not been widely investigated for the power-domain downlink OTFS-NOMA system. Motivated by this, we provide a thorough description of the OTFS-NOMA scheme for high mobility users in this manuscript, including its system architecture, channel model, numerical results with delays, Doppler effect, and modulation types.

The study consists of the following sections. In the second section of this study, the OTFS-NOMA system scheme is demonstrated. In this section, the OTFS-NOMA system model, TF domain, DD domain, channel model, and general principles of OTFS are described. In the third section of this study, the BER performance for the proposed system model and numerical results are presented. Finally, the conclusion is given in Section 4.

2. OTFS-NOMA System Model

In the OTFS-based power domain NOMA system model, users with high-speed mobility use the same DD domain source with different transmission power. As seen in Figure 1, an OTFS-based downlink NOMA system model with source T, two destination users namely near the user and from the user, U_i, $i \in \{1,2\}$, the number of users, $K = 2$, and reflectors are investigated. The received signal is the sum of delayed, attenuated, and Doppler-shifted copies for the destination users. The delay is a function of the length of each propagation path, while the Doppler shift is a result of the relative motion of the receiver and reflectors for the case where the transmitter is considered stationary.

2.1 TF Domain and DD Domain

OTFS-NOMA uses both the TF domain and the DD domain efficiently. By sampling with time interval T and frequency interval Δf, a discrete TF domain is obtained as seen in Equation 1

$$\Lambda_{TF} = \{(nT, m\Delta f), n = 0, \cdots, N-1, m = 0, \cdots, M-1\}, \quad (1)$$

where $N, M > 0$ [10], [11]. Accordingly, the discrete DD domain is as seen in Equation 2

$$\Lambda_{DD} = \left\{\left(\frac{k}{NT}, \frac{l}{M\Delta f}\right), k = 0, \cdots, N-1, l = 0, \cdots, M-1\right\}, \quad (2)$$

where N and M are the total number of time intervals and frequency subcarriers.

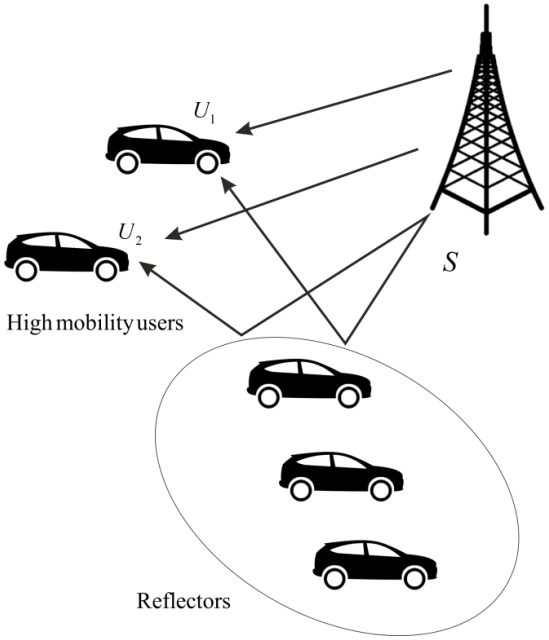

Figure 1 OTFS-based power domain NOMA System Model

2.2 Channel Model

In a multi-user mobility communication network where the transmitter communicates with K users, τ delay, υ Doppler shift, $h_i(\tau, \upsilon)$ indicates the channel response for $1 \leq i \leq K$, in the DD domain. OTFS facilitates channel estimation and signal detection by using the wireless channel sparsity in the DD domain. As a result, it is considered that there are a few propagation paths between transmitter and receiver. As seen in Equation 3, the channel impulse response is defined in a DD domain as

$$h_i(\tau, \upsilon) = \sum_{p=1}^{P_i} h_{i,p}\delta(\tau - \tau_{i,p})\delta(\upsilon - \upsilon_{i,p}), \quad (3)$$

where P_i is the number of propagation paths between the transmitter and user i, $h_{i,p}$ is the independent and uniformly distributed (i.i.d) complex Gaussian channel gain, $\tau_{i,p}$ is the delay in the propagation path, $\upsilon_{i,p}$ is the Doppler shift in the propagation path and δ indicates the Dirac delta function. Each user has a total power of 1, where the channel gain $h_{i,p} \sim C\,N\,(0, \frac{1}{P_i})$. $\frac{1}{M\Delta f}$ and $\frac{1}{NT}$ are delay and Doppler resolution of OTFS, respectively.

2.3 General Principles of OTFS

OTFS general modulation/demodulation block diagram is given as seen in Figure 2. $x[k, l]$ information bits are transmitted as $M \times N$ QAM symbols. The inverse symplectic fast Fourier transform (ISFFT) is then applied to convert the DD domain signal $x[k, l]$ into the TF domain signal $X[n, m]$. After applying the Heisenberg transformation to the $x[n, m]$ matrix, the $s(t)$ signal is obtained and transmitted to the communication channel. At the receiver, the Wigner transform is first applied to the time domain signal $r(t)$ to obtain the TF domain signal $Y[n, m]$. In the demodulation part, a symplectic fast Fourier transform (SFFT) is employed to obtain the DD domain signal $y[k, l]$. Finally, the signals are detected by applying the MP detection method [12]. This algorithm performs detection based on the SIC principle and alternates the decision outputs iteratively [13].

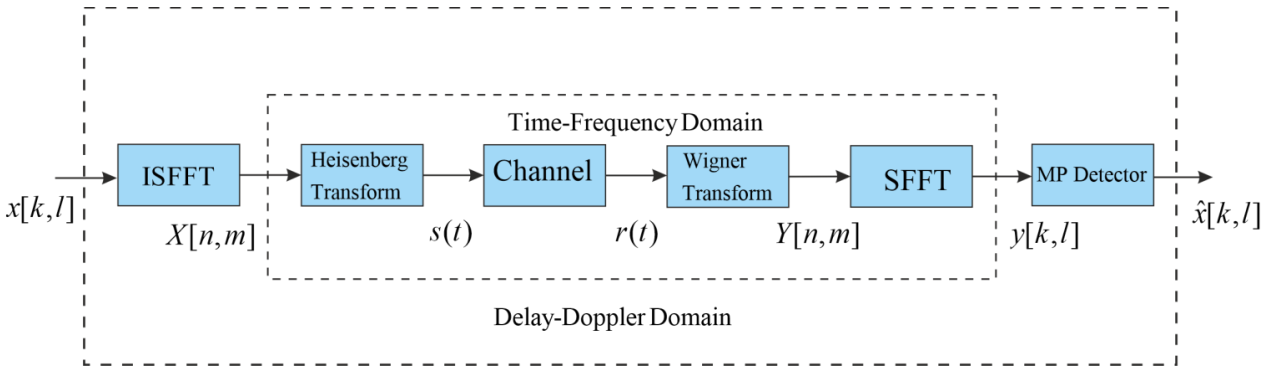

Figure 2 OTFS General Modulation/Demodulation Block Diagram

The symbols $x_i[k,l]$ in the DD domain for the *i*-th mobile user transmitted by the OTFS transmitter can be formulated as the signal $X_i[n,m]$ in the TF domain as seen in Equation 4

$$X_i[n,m] = \frac{1}{\sqrt{NM}} \sum_{k=0}^{N-1} \sum_{l=0}^{M-1} x_i[k,l] e^{j2\pi\left(\frac{nk}{N} - \frac{ml}{M}\right)}, \tag{4}$$

where $x_i[k,l]$ represents the matrix for the *i*-th user and $n = 0, \cdots, N-1, m = 0, \cdots, M-1$ [11]. Then, a continuous time signal is created by applying the Heisenberg transform to the TF signal matrix $X_i[n,m]$. The *i*-th NOMA user's signal is as seen in Equation 5

$$s_i(t) = \sum_{n=0}^{N-1} \sum_{m=0}^{M-1} (\sqrt{\xi_i \alpha_i} X_i[n,m] g_{tx}(t-nT) e^{j2\pi m\Delta f(t-nT)}, \tag{5}$$

where ξ_i is the transmission power of *i*-th user, $T = 1/\Delta f$ is the symbol duration, $g_{tx}(t)$ is the transmit pulse shaping waveform while α_i indicates the power allocation coefficient for destination users and $\sum_{i=0}^{K} \alpha_i = 1$. For the far user, high priority is given due to the quality-of-service requirement, $\alpha_2 > \alpha_1$. The signal $s_i(t)$ is transmitted over a channel $h_i(\tau, \upsilon)$ with a channel impulse response, resulting in the signal $r_i(t)$ as seen in Equation 6

$$r_i(t) = \iint h_i(\tau,\upsilon) s_i(t-\tau) e^{j2\pi\upsilon(t-\tau)} d\tau d\upsilon + w_i(t), \tag{6}$$

where $w_i(t)$ indicates the complex additive white Gaussian noise (AWGN) and σ_i^2 is the variance. The received signal $r_i(t)$ is sampled with period T_s $(t = qT_s, q = 0, \ldots, NM-1)$ and received discrete signal samples are as seen in Equation 7

$$r_i[q] = \sum_{l=0}^{L-1} h_i[q,l]\, s_i[q-l] + w_i[n], \tag{7}$$

where $h_i[q,l]$ is the channel impulse response of the *i*-th user. Here, q is the instant time and l is the delay. The discrete-time signal for the *i*-th user is received within a matrix as $\boldsymbol{r_i} = \boldsymbol{H_i} s + \boldsymbol{w}_i$ where $\boldsymbol{w_i}$ is $MN \times 1$ complex AWGN vector and $\boldsymbol{H_i}$ is the $MN \times MN$ channel matrix of *i*-th user generated from the impulse responses. At the receiver, the following cross-ambiguity function is first calculated in a matched filter as seen in Equation 8

$$Y_i(t,f) = \int g_{rx}^*(t'-t) r_i(t') e^{-j2\pi f(t'-t)} dt', \tag{8}$$

where $g_{rx}^*(t)$ represents the received waveform. As seen in Equation 9, it is possible to acquire the output of the matched filter by sampling $Y(t,f)$ as

$$Y_i[n,m] = Y_i(t,f)|_{t=nT, f=m\Delta f}. \tag{9}$$

Equations 8 and 9 denote the Wigner transformation. Then, SFFT is applied to $Y_i[n,m]$ samples and the symbols $y_i[k,l]$ are obtained in the DD domain as

$$y_i[k,l] = \frac{1}{\sqrt{NM}} \sum_{n=0}^{N-1} \sum_{m=0}^{M-1} Y_i[n,m] e^{-j2\pi\left(\frac{nk}{N} - \frac{ml}{M}\right)}. \quad (10)$$

Here, we assume the orthogonality between transmitted and received pulses. The received signal is modeled as seen in Equation 11

$$Y_i[n,m] = H_i[n,m]X_i[n,m] + W_i[n,m], \quad (11)$$

where $W_i[n,m]$ represents AWGN in the TF domain and $H_i(n,m) = \iint h_i(\tau,\upsilon) e^{j2\pi\upsilon nT} e^{-j2\pi(\upsilon+m\Delta f)\tau} d\tau d\upsilon$. Ultimately, the transmitted signal will be recovered as $\hat{x}[k,l]$ by signal detection and demodulation [14].

3. Numerical Results

The BER performance of the power domain downlink OTFS-NOMA simulation results under Rayleigh fading distribution with 4-QAM/16-QAM modulation is presented in this section. The PA coefficient is assumed to be 0.85 for the far user and 0.15 for the near user. The simulation parameters are listed as seen in Table 1. The BER performance is based on the assumption that the destination users move at a maximum speed of 380.7 km/h. Here, the number of propagation paths is taken as $P_i = 4$ and the DD grid size is $M = 32, N = 32$.

Table 1 Simulation Parameters

Parameter	Value
Number of paths (P_i)	4
Carrier Frequency (f_c)	4 Ghz
Subcarrier Spacing (Δf)	15 kHz
Modulation Alphabet	4-QAM/ 16-QAM
Max Speed (Kmph)	380.7
Delay-Doppler Grid Size	$M, N = 32, 32$
Symbol duration ($T = 1/\Delta f$)	0.0667 ms

The carrier frequency offset is represented as $f_D = v\ f_c/c$, where f_c is the carrier frequency, c is the speed of the light and v is the speed of the movement between the transceivers [15]. As seen in Table 2, it is considered that the maximum Doppler is set to 1410 Hz, and velocity is set to 380.7 km/h at a carrier frequency of 4 GHz. The maximum multi-path delay is set to 8.4 μs [16].

Table 2 Delay and Doppler Models

Path index(p)	1	2	3	4
Delay ($\tau_i, \mu s$)	2.1	4.2	6.3	8.4
Doppler (υ_i, Hz)	0	470	940	1410

As seen in Figures 3 and 4 demonstrate the BER values derived from the MP detection algorithm based on the signal-to-noise ratio (SNR). Figure 3 demonstrates the BER performance analysis that varies with SNR for both destination users. In this figure, we assume that the modulation type is 4-QAM and OTFS frame size is $M = 32$, $N = 32$. It is observed that the performance of the far user did not drop below a particular BER level as expected. It is assumed that the far user recognizes the interference caused by the near user as noise and is unable to decode. It is seen that the BER value for the U_1 user is 0.1, while the BER value for the U_2 user is nearly 0.25 at 10 dB SNR, resulting in 2.5 times better BER performance. Furthermore, the improvement in BER in U_1 is better than in U_2 as SNR increases.

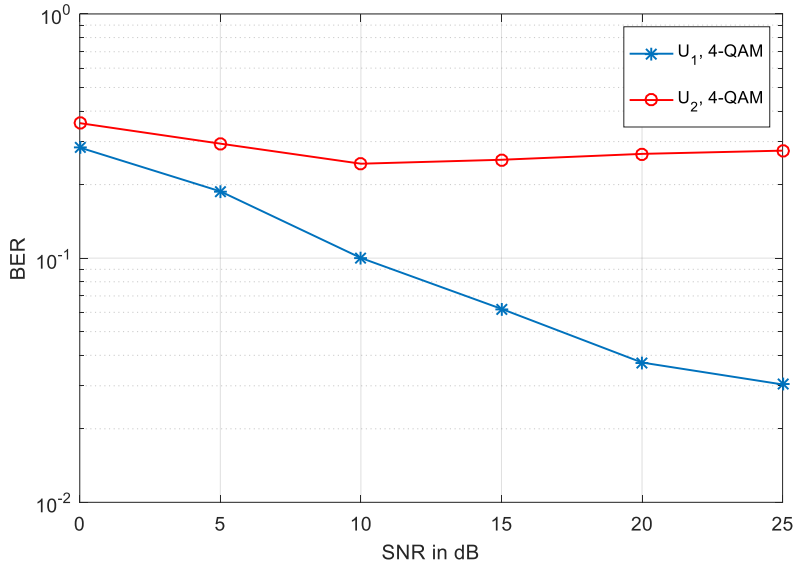

Figure 3 BER Evaluation for the OTFS-NOMA (4-QAM, $M = 32$, $N = 32$)

Figure 4 examines the BER performance for the OTFS-NOMA for both near and far users varying with SNR under 16-QAM modulation and OTFS frame size of $M = 32$, $N = 32$. It is observed that the Doppler effect causes the BER performance of both users to become poorer. It is apparent that the BER value is nearly 0.27 for the U_1 user, while the BER value for the U_2 user is approximately 0.33 at 10 dB SNR, resulting in a better BER performance. Thus, the improvement in BER in U_1 is better than in U_2 as SNR increases. Simulation results with 16-QAM show worse results than the BER performance obtained with 4-QAM. This is a conclusion that can be drawn from both figures. This result has also been observed in a similar study documented in the literature [17].

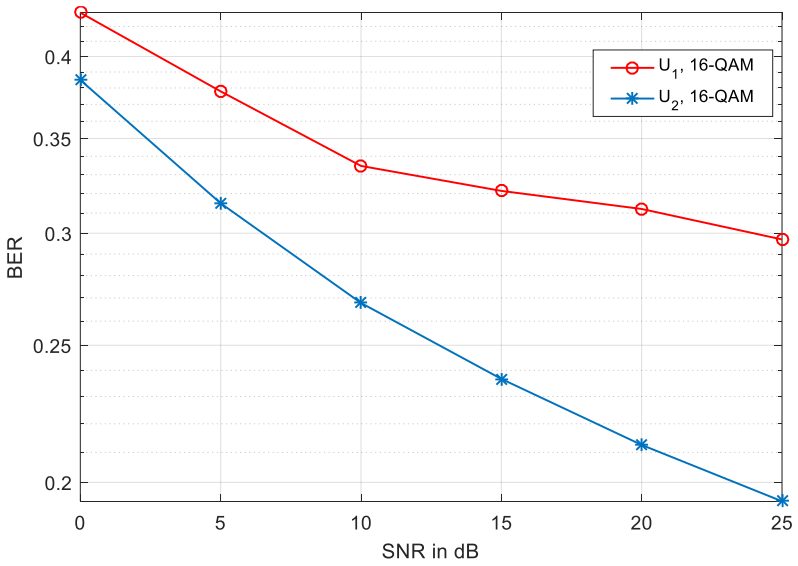

Figure 4 BER Evaluation for the OTFS-NOMA (16-QAM, $M = 32$, $N = 32$)

4. Conclusions

In this work, the BER performance is analyzed for the power-domain downlink OTFS-NOMA system model with high-speed mobility. In the BER simulation results, PA coefficient, delays, and Doppler effects caused by the velocity parameters of the users in motion are taken into consideration. In the proposed OTFS-NOMA system, the message passing detection algorithm is utilized to analyze the BER performance for destination users. It is observed that reflections and delays from users at higher velocities reduce the system performance. It is noted that the far user's performance did not deteriorate below a specific BER threshold. In the 4-QAM situation, the BER performance is 2.5 times higher for the U_1 user (BER value = 0.1) than for the U_2 user (BER value = approximately 0.25 at 10 dB SNR). In the 16-QAM technique,

the BER value for the U_1 user is around 0.27, while the BER value for the U_2 user is roughly 0.33 at 10 dB SNR. It is observed that both users' BER performance degrades due to the Doppler effect.

Although we investigated the BER performance for OTFS modulated NOMA system for two destination users in the high mobility environment, it is possible to extend the provided analysis to more generalized results for the enabling technologies in 6G wireless networks, such as unmanned aerial vehicles (UAVs) [18-21], reflecting intelligent surfaces (IRS), non-terrestrial networks, and integrated sensing and communications (ISAC). Integrating these enabling technologies for OTFS-based NOMA will be a promising way to enhance the functionality of our future study. Besides, cognitive radio [22-23] architecture will be a different solution scenario. Secondary user signal detection algorithms to increase the spectral efficiency [24] for high-speed mobile environments may be another topic of our study. In addition, reliability, secrecy performance analysis, and channel estimation schemes are planned to work on OTFS modulated NOMA systems.

References

[1] I. Umakoglu, M. Namdar, A. Basgumus, F. Kara, H. Kaya, and H. Yanikomeroglu, "BER Performance Comparison of AF and DF Assisted Relay Selection Schemes in Cooperative NOMA Systems," *IEEE 9th International Black Sea Conference on Comm. and Networking*, Bucharest, Romania, 2021.

[2] Z. Ding, M. Peng, and H.V. Poor, "Cooperative non-orthogonal multiple access in 5G systems," *IEEE Comm. Lett.*, vol. 19, no. 8, pp. 1462–1465, 2015.

[3] Y. Saito, A. Benjebbour, Y. Kishiyama, and T. Nakamura, "System level performance evaluation of downlink non-orthogonal multiple access (NOMA)," *in Proc. IEEE 24th Annu. Int. Symp. Pers., Indoor, Mobile Radio Comm.*, London, U.K., Sep. 2013, pp. 611–615.

[4] Z. Ding, Z. Yang, P. Fan, and H. V. Poor, "On the performance of nonorthogonalmultiple access in 5G systems with randomly deployed users," *IEEE Signal Process. Lett.*, vol. 21, no. 12, pp. 1501–1505, Dec. 2014.

[5] S. McWade, M. F. Flanagan, A. Farhang, "Low-Complexity Equalization and Detection for OTFS-NOMA", arXiv preprint arXiv:2211.07388, 2022.

[6] G. D. Surabhi, R. M. Augustine, A. Chockalingam, "Multiple access in the delay-Doppler domain using OTFS modulation," arXiv preprint, 2019.

[7] Z. Ding, R. Schober, P. Fan, and H. Vincent Poor, "OTFS-NOMA: An Efficient Approach for Exploiting Heterogenous User Mobility Profiles," IEEE Transactions on Comm., vol. 67, no. 11, pp. 7950–7965, 2019.

[8] A. Chatterjee, V. Rangamgari, S. Tiwari, and S. S. Das, "Nonorthogonal Multiple Access With Orthogonal Time–Frequency Space Signal Transmission," IEEE Systems Journal, vol. 15, no. 1, pp. 383–394, 2021.

[9] K. Deka, A. Thomas, and S. Sharma, "OTFS-SCMA: A Code-Domain NOMA Approach for Orthogonal Time Frequency Space Modulation," *IEEE Transactions on Comm.*, vol. 69, no. 8, pp. 5043–5058, 2021.

[10] H. Wen, W. Yuan, and S. Li, "Downlink OTFS Non-Orthogonal Multiple Access Receiver Design based on Cross-Domain Detection," *in IEEE International Conference on Comm. Workshops*, 2022, pp. 928–933.

[11] P. Raviteja, K. T. Phan, Y. Hong and E. Viterbo, "Interference Cancellation and Iterative Detection for Orthogonal Time Frequency Space Modulation," *in IEEE Transactions on Wireless Comm.*, vol. 17, no. 10, pp. 6501-6515, 2018, doi: 10.1109/TWC.2018.2860011.

[12] L. Xiao, S. Li, Y. Qian, D. Chen and T. Jiang, "An Overview of OTFS for Internet of Things: Concepts, Benefits, and Challenges," *in IEEE Internet of Things Journal*, vol. 9, no. 10, pp. 7596-7618, 2022, doi: 10.1109/JIOT.2021.3132606.

[13] H. Zhang, K. Niu, J. Xu, J. Dai and J. Zhang, "Iterative SIC-Based Multiuser Detection for Uplink Heterogeneous NOMA System," *2022 IEEE Globecom Workshops*, Rio de Janeiro, Brazil, 2022, pp. 94-99.

[14] I. Umakoglu, M. Namdar, A. Basgumus, S. Özyurt and S. Kulaç, "BER Performance Analysis for NOMA Systems with OTFS Modulation," *2023 31st Signal Process. and Comm. Appl. Conference*, Istanbul, Turkiye, 2023, pp. 1-4.

[15] Y. Zhang, S. Zhang, B. Wang, Y. Liu, W. Bai and X. Shen, "Deep Learning-Based Signal Detection for Underwater Acoustic OTFS Communication, " *Journal of Marine Science and Engineering*, vol. 10, no. 12, 2022.

[16] T. Thaj and E. Viterbo, "Low-Complexity Linear Diversity-Combining Detector for MIMO-OTFS," in *IEEE Wireless Comm. Lett.*, vol. 11, no. 2, pp. 288-292, Feb. 2022, doi: 10.1109/LWC.2021.3125986.

[17] K. Yadav, P. Singh, H.B. Mishra, and R. Budhiraja, "Closed Form BER For ZF OTFS Receivers," *IEEE 22nd International Workshop on Signal Processing Advances in Wireless Communications*, 2021.

[18] I. Umakoglu, M. Namdar, and A. Basgumus, "UAV-Assisted Cooperative NOMA System with the nth Best Relay Selection," *Advances in Electrical and Computer Engineering*, vol. 23, no. 3, pp. 39-46, 2023.

[19] T. Yılmaz, A.A. Bacanlı, and H. İlhan, "UAV-Assisted NOMA-Based Network with Alamouti Space-Time Block Coding," *Politeknik Dergisi*, vol. 25 no. 3, pp. 967-973, 2022.

[20] S. Koşu, and S.Ö. Ata, "NOMA-enabled Cooperative V2V Communications with Fixed-Gain AF Relaying," *Balkan Journal of Electrical and Computer Engineering*, vol. 11, no. 1, pp. 1-12, 2023.

[21] A. Basgumus, F. Kocak, and M. Namdar, "BER performance analysis for downlink NOMA systems over cascaded Nakagami-m fading channels," *Annals of Telecommunications*, 1-7, 2023.
[22] F.K. Bardak, M. Namdar, and A. Basgumus, "Ergodic Capacity Analysis of the Relay Assisted Downlink NOMA Systems in Cognitive Radio Networks," *Journal of Engineering Sciences and Design*, vol. 9, no. 3, pp. 992-1002, 2021.
[23] M. Namdar, A. Guney, F.K. Bardak, and A. Basgumus, "Ergodic Capacity Estimation with Artificial Neural Networks in NOMA-Based Cognitive Radio Systems" *Arabian Journal for Science and Engineering*, 1-10, 2023.
[24] A. Basgumus, M. S. Ardic, and M. Namdar, "Capacity Analysis of the Secondary Users in Spectrum Sharing Model over Nakagami-m and log-normal Fading Channels," *Journal of the Faculty of Engineering and Architecture of Gazi University*, vol. 38, no. 4, pp. 2205-2212, 2023.

Conflict of Interest Notice
The authors declare that there is no conflict of interest regarding the publication of this paper.

Ethical Approval and Informed Consent
It is declared that during the preparation process of this study, scientific and ethical principles were followed, and all the studies benefited from are stated in the bibliography.

Availability of data and material
Not applicable.

Plagiarism Statement
This article has been scanned by iThenticate ™.